

**Electronic Supplementary Information**

**Control of Hydration Layer States on Phosphorus-containing Mesoporous Silica Films and Their Reactivity Evaluation with Biological Fluid**

Shota Yamada,<sup>1,2</sup> Takaki Kobashi,<sup>1</sup> Motohiro Tagaya<sup>1,\*</sup>

<sup>1</sup> Department of Materials Science and Technology, Nagaoka University of Technology,  
Kamitomioka 1603-1, Nagaoka, Niigata 940-2188, Japan

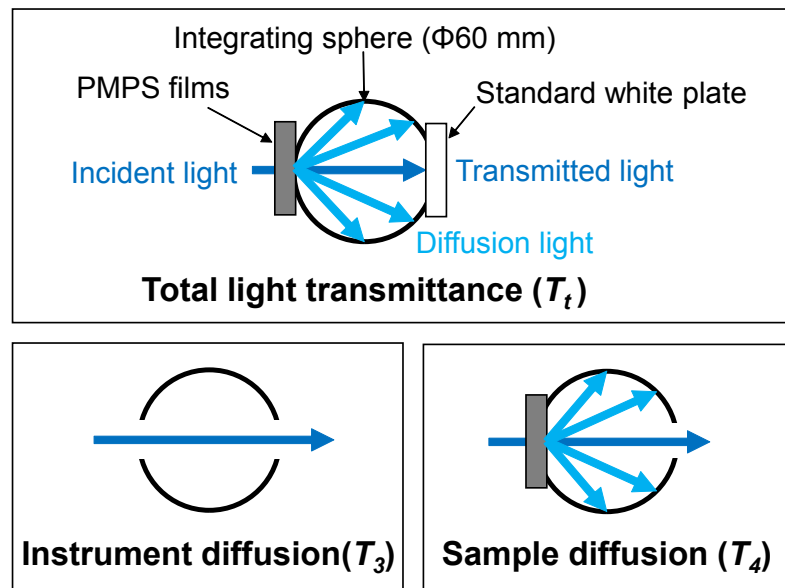
<sup>2</sup> Japan Society for the Promotion of Science,  
5-3-1 Koji-machi, Chiyoda-ku, Tokyo 102-0083, Japan

---

\* Author to whom correspondence should be addressed:

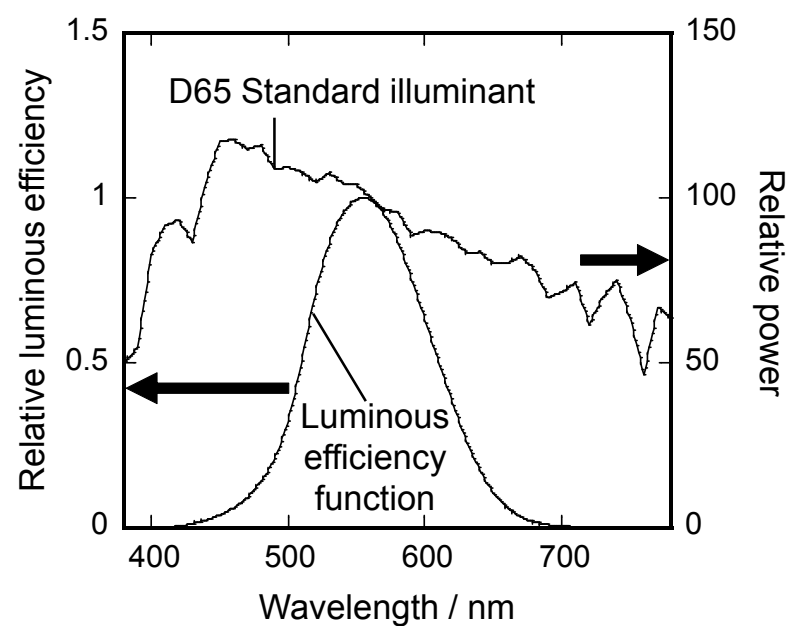
Tel: +81-258-47-9345; Fax: +81-258-47-9300, E-mail: tagaya@mst.nagaokaut.ac.jp

**Scheme S1**



**Scheme S1.** Illustration of the haze value measurement setup using the total transmittance ( $T_t$ ), the instrument diffusion ( $T_3$ ) and the sample diffusion rate ( $T_4$ ) inside the integrating sphere.

**Scheme S2**



**Scheme S2.** Spectra of luminous efficiency functions and D65 standard illuminant.

**Figure S1**

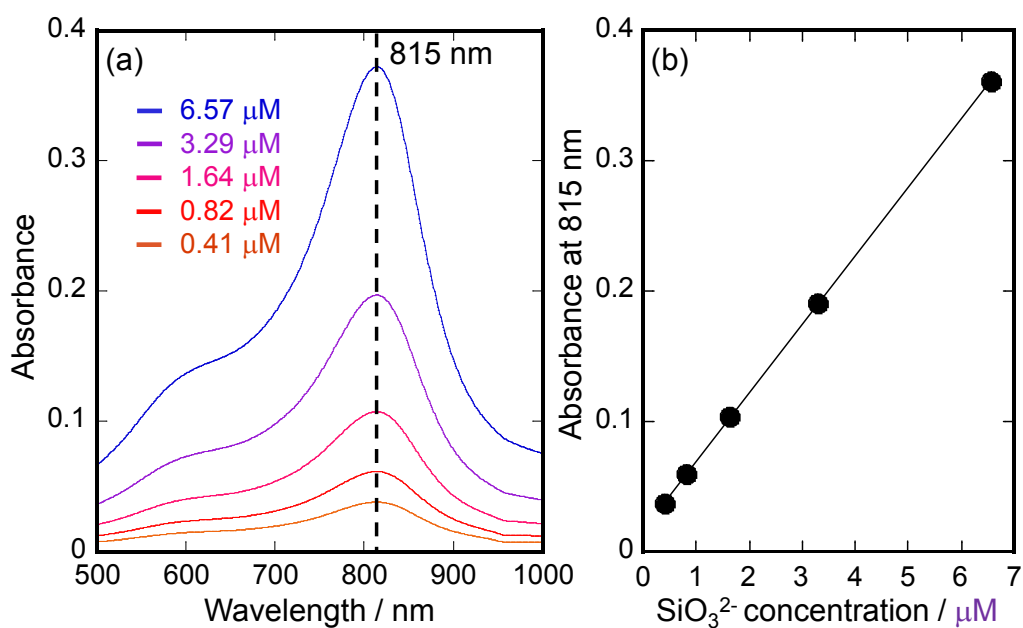


**Figure S1.** (a) UV-Vis absorption spectra of the molybdenum-blue-staining for  $\text{SiO}_3^{2-}$  in PB with the different concentrations, and (b) their calibration curve between the concentration and absorbance ( $R=0.9999$ ).

**Figure S2**

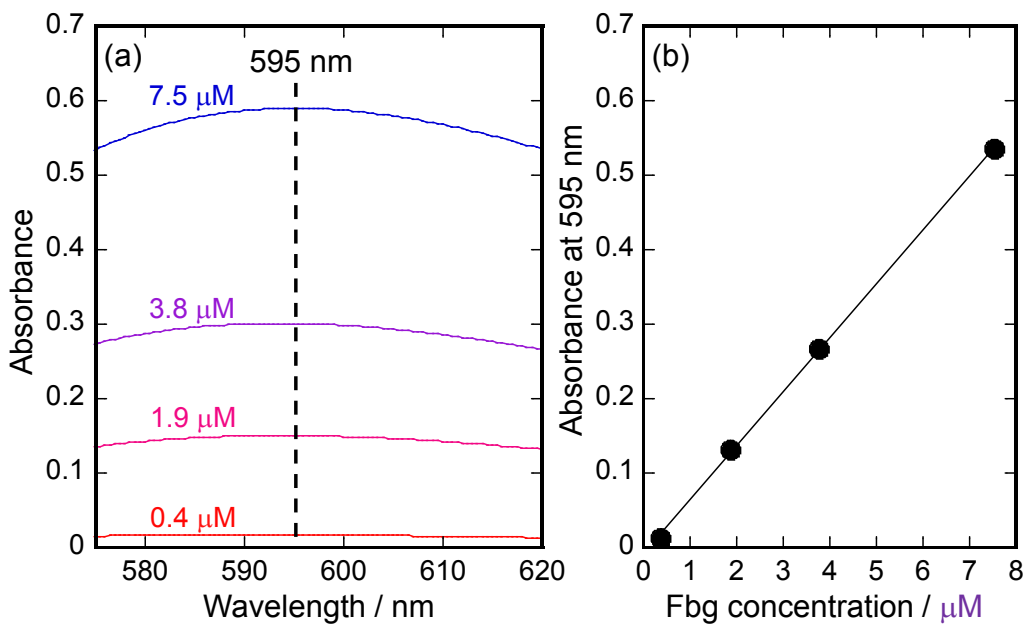


**Figure S2.** (a) UV-Vis absorption spectra of the Fbg in PB with the different concentrations, and (b) their calibration curve between the concentration and absorbance ( $R=0.9998$ ).

**Figure S3**

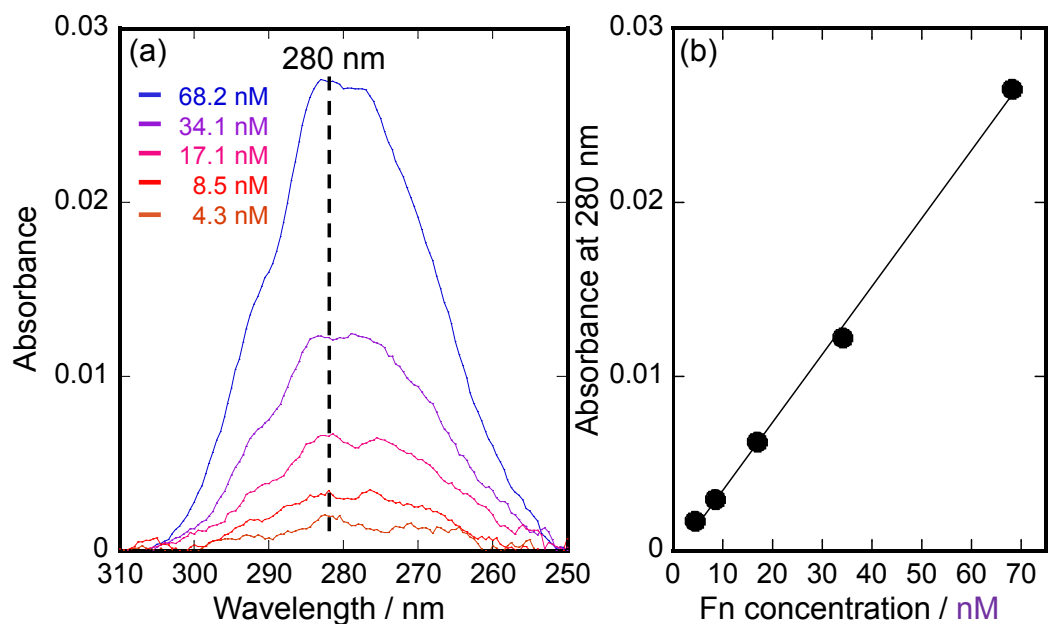
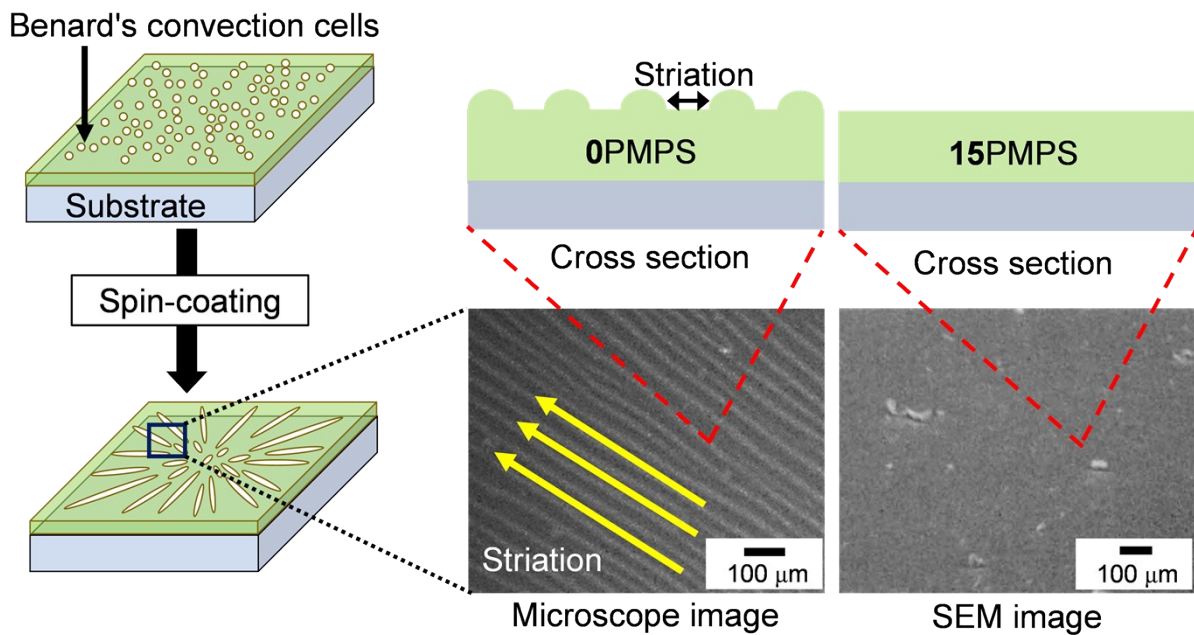


**Figure S3.** (a) UV-Vis absorption spectra of the Fn in PB with the different concentrations, and (b) their calibration curve between the concentration and absorbance ( $R=0.9991$ ).

**Scheme S3**



**Scheme S3.** Illustration of the possible striped pattern (i.e., striation structure) formation process of **0PMPS** surface by Marangoni effect in the spin-coating and the surface structure observed by the optical microscope, and the **15PMPS** surface structure observed by SEM.

**Figure S4**

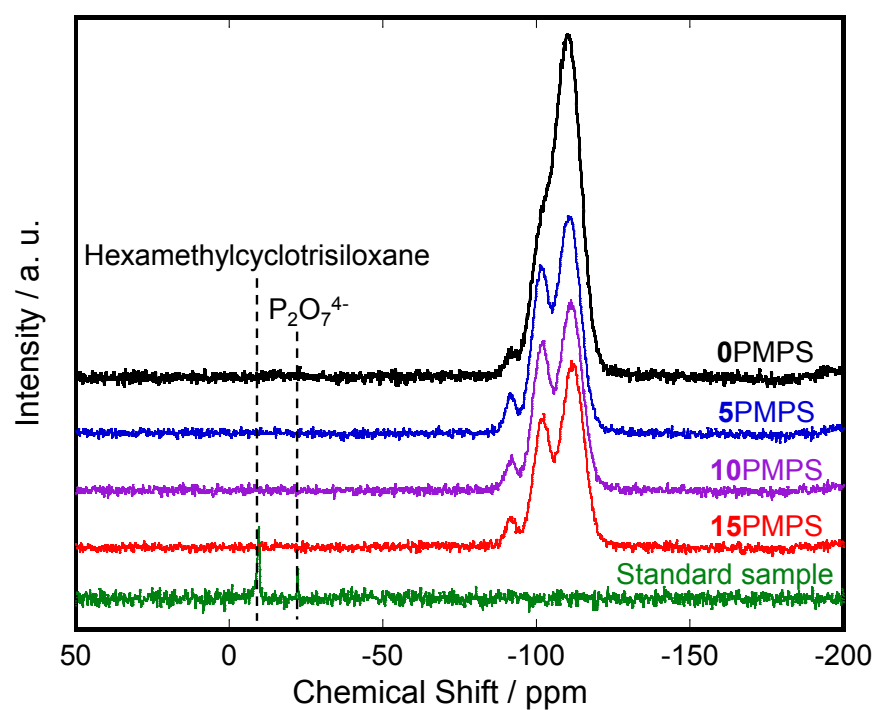


**Figure S4.** Solid-state  $^{29}\text{Si}$ -NMR DD/MAS spectra of the PMPS films. (standard sample: hexamethylcyclotrisiloxane).

**Figure S5**

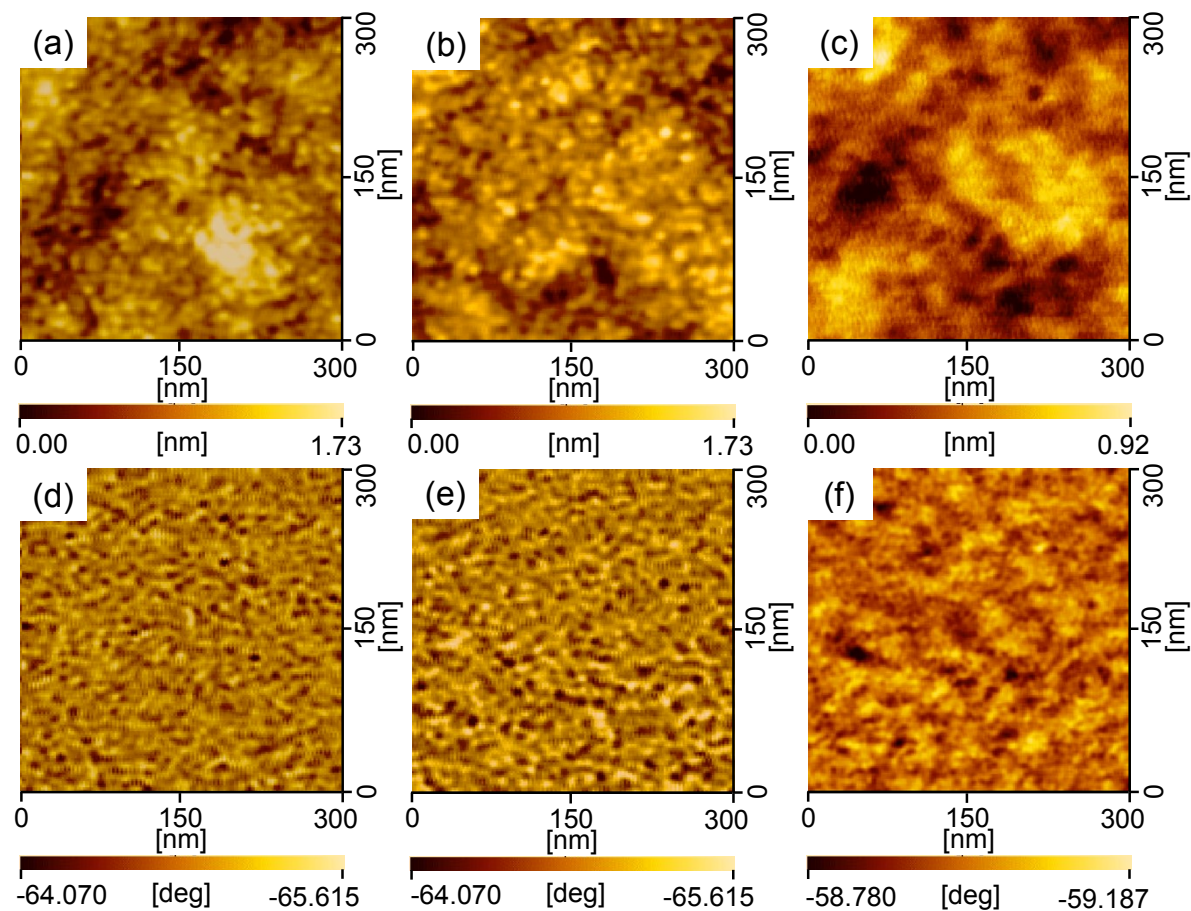


**Figure S5.** AFM (a–c) topographic and (d–f) phase-shift images of the (a, d) 0PMPS, (b, e) 15PMPS and (c, f) Si wafer.

**Figure S6**

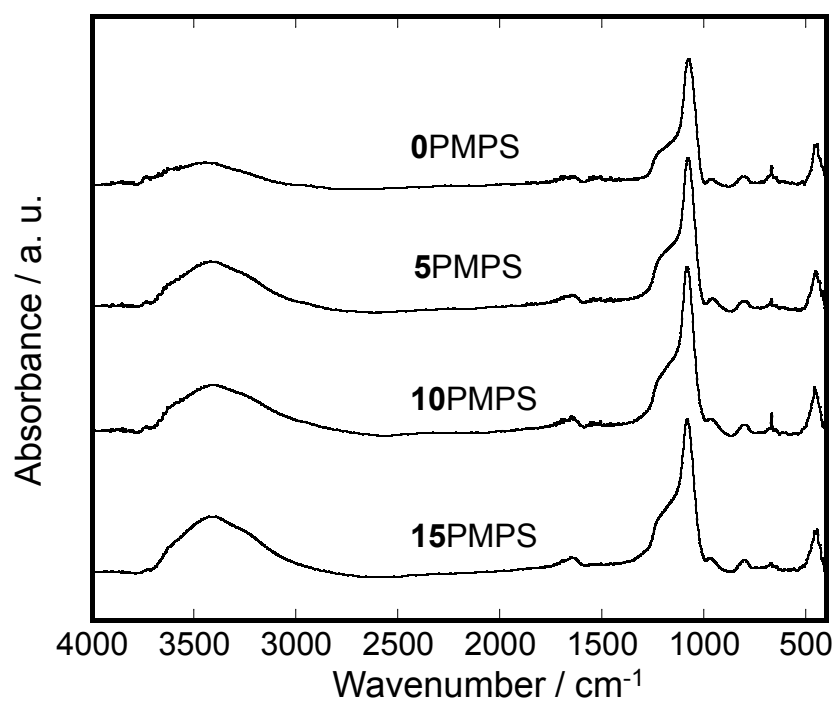


**Figure S6.** FT-IR spectra of the PMPS films.

**Table S1****Table S1.** Absorption band assignments of the FT-IR spectra of the PMPS films.

Wavenumber / cm <sup>-1</sup>	Attribution	Bonding state
450	Si–O–Si	Rocking
	P–O–P	Rocking
801	Si–O–Si	Bending
950	Si–OH	Symmetric stretching
	P–O–P	Asymmetric stretching
1080	Si–O–Si	Symmetric stretching
1140	Si–O–P	Stretching
1200	Si–O–Si	Asymmetric stretching
	P–O–P	Symmetric stretching
1463	P=O	Stretching
1652	H–O–H	Bending
2800	–OH in O=P–OH	Stretching
3420	–OH in Water	Stretching
3650	Si–OH	Stretching

**Figure S7**

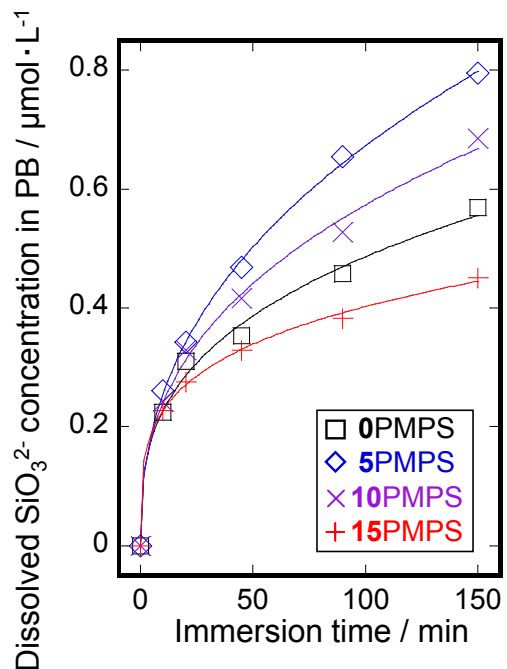


**Figure S7.** Dissolved  $\text{SiO}_3^{2-}$  concentration from the PMPS films into PB with the immersion time.

**Figure S8**

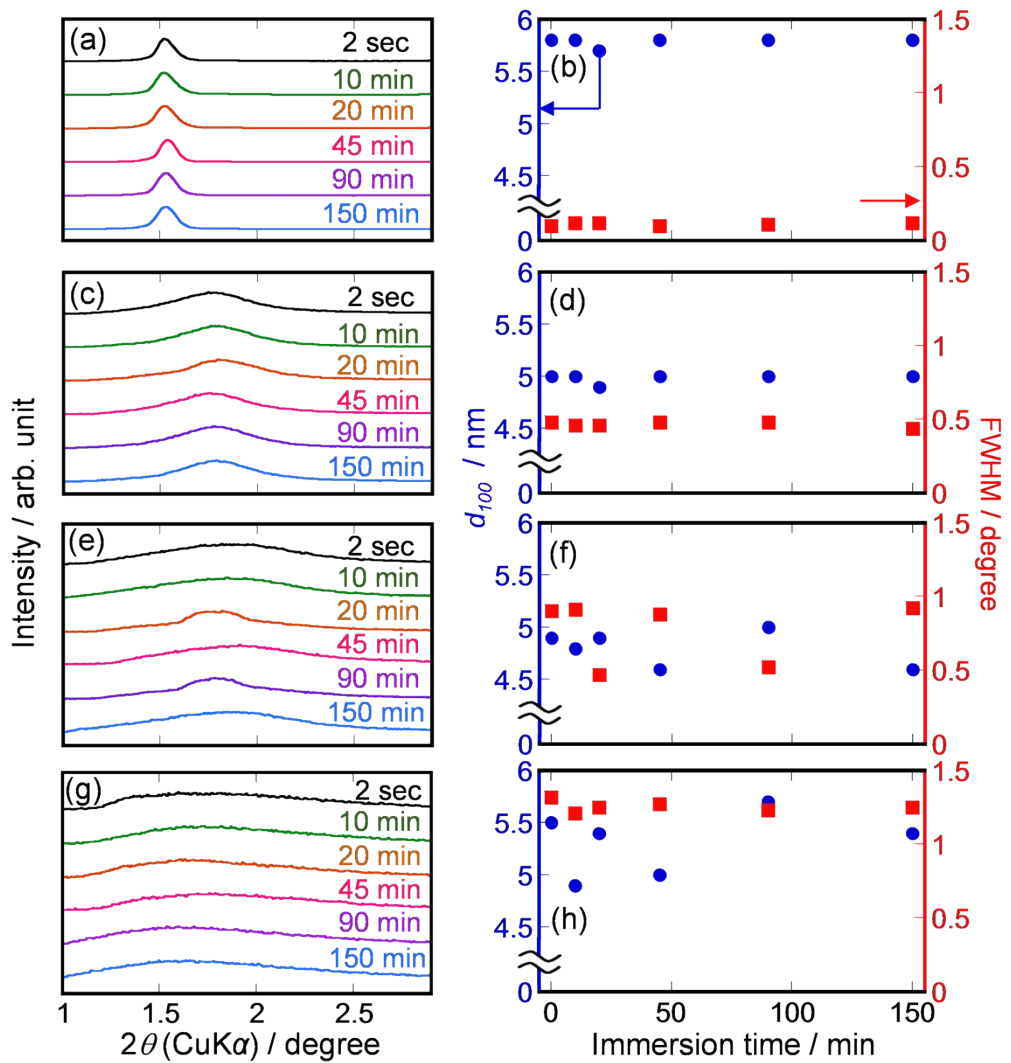


**Figure S8.** (a, c, e, g) XRD patterns and (b, d, f, h)  $d_{100}$  (nm) and FWHM (degree) of (a,b) 0PMPS, (c,d) 5PMPS, (e,f) 10PMPS and (g,h) 15PMPS at the different immersion times.

**Figure S9**

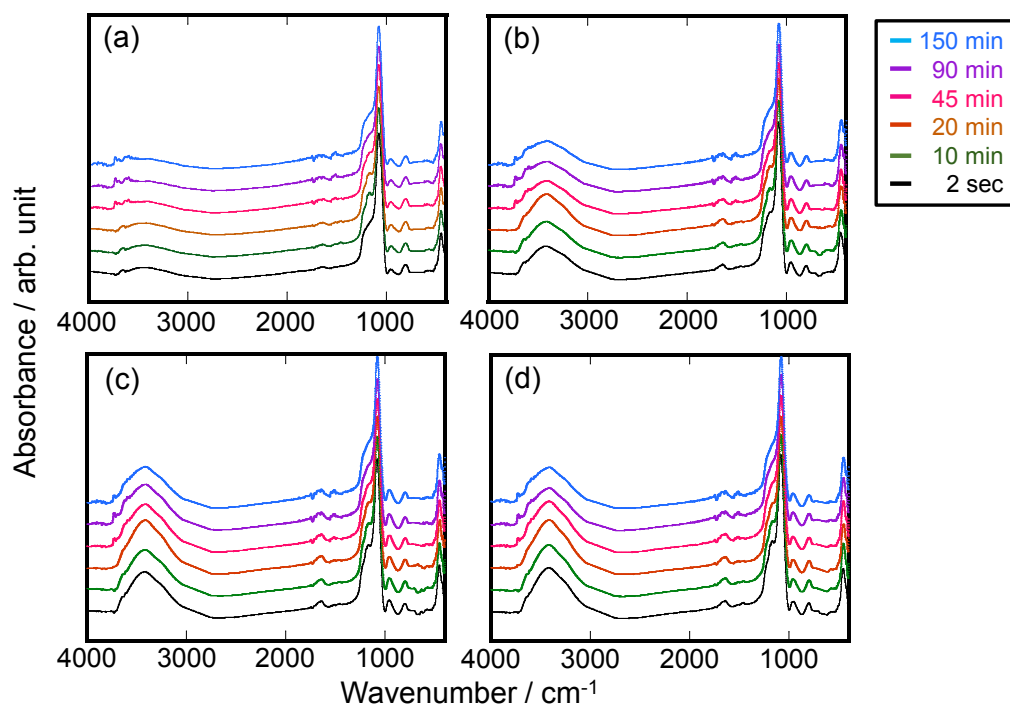


**Figure S9.** FT-IR spectra of (a) **0PMPS**, (b) **5PMPS**, (c) **10PMPS** and (d) **15PMPS** at the different immersion times.